RSC Advances

ROYAL SOCIETY OF CHEMISTRY

www.rsc.org/advances

Table of contents entry

Synthetic scorpiand-like azamacrocycles selectively inhibit SOD and TR enzymes of *Trypanosoma cruzi* causing parasites death and increasing the mice survival after infection and treatment.

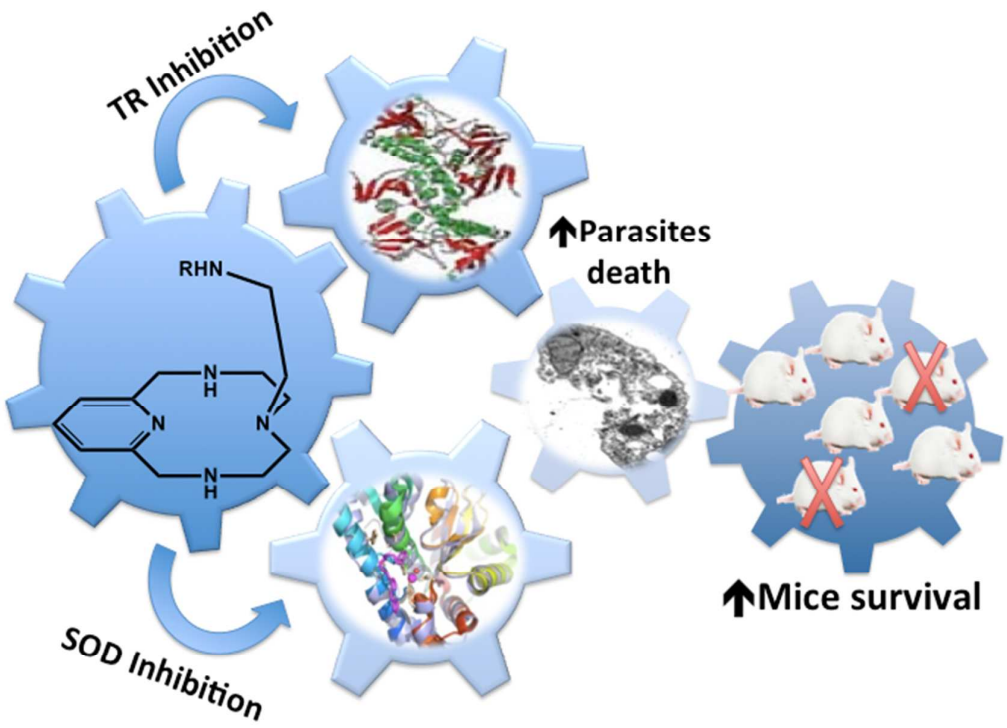

Journal Name

RSCPublishing

ARTICLE

Synthetic single and double *aza-scorpiand* macrocycles act as inhibitors of the antioxidant enzymes iron superoxide dismutase and trypanothione reductase in *Trypanosoma cruzi* with promising results in a murine model.

Cite this: DOI: 10.1039/x0xx00000x

Received ooth January 2012,
Accepted ooth January 2012

DOI: 10.1039/x0xx00000x

www.rsc.org/

F. Olmo,[a] M. P. Clares,[b] C. Marín,[a] J. González,[b] M. Inclán,[b] C. Soriano,[c] K. Urbanová,[a] R. Tejero,[d] M. J. Rosales,[a] R.L. Krauth-Siegel,[e] M. Sánchez-Moreno,[a,*] and E. García-España.[b,*]

The anti-chagasic activity of a series of eleven derivatives of aza-scorpiand-like macrocycles, some of them newly synthesised, was assayed. The four compounds with the best selectivity indices *in vitro* were subjected to *in vivo* assays. Tests in a murine model of the acute phase of Chagas disease showed a two-fold reduction in parasitaemia compared to that with benznidazole. Furthermore, compounds **7** and **11,** with 4-pyridine and phenanthroline substituents in the lateral chain, caused a remarkable decrease in parasitaemia reactivation during the chronic phase after inducing immunosuppression in mice. These activity studies were complemented by measuring their inhibitory effect towards the antioxidant parasite-specific enzymes Fe-superoxide dismutase (Fe-SOD) and trypanothione reductase (TR), the metabolites excreted after treatment and ultrastructural alterations. The ability of selected macrocycles to complex with Fe(II) and Fe(III) was studied by potentiometric methods. Detailed molecular dynamics studies provided interesting hints about the way in which the compounds approach and modify the active centre of Fe-SOD. The activity, low toxicity, stability, low cost of the starting materials and straightforward synthesis make these compounds appropriate molecules for the development of affordable anti-chagasic agents.

Introduction

Chagas disease (CD) is a chronic, systemic, parasitic infection caused by the protozoan *Trypanosoma cruzi*[1] and is identified by the WHO as one of the world's 17 most neglected tropical diseases.[2] This disease represents one of the main public health concerns in 21 countries in Latin America where about 7-8 million people are currently infected with *T. cruzi*.[3] Actually, CD is becoming an emerging health problem in non-endemic areas, since the parasite has travelled outside of South and Central America because of population migration (North America, Pacific region and Europe). Thus, CD is becoming a new worldwide epidemiological, economic, social and political challenge. However, as reported by the WHO, whereas research funding to combat HIV/AIDS, malaria and tuberculosis (TB) has been considerably increased in the last years, that devoted to attend other infectious diseases associated with poverty, such as CD, has not been increased in the same manner.[4]

Currently, the main drugs used to treat Chagas disease are two nitroaromatic heterocycles: the furane-based nifurtimox and the imidazole-based benznidazole (Bz).[5] Both drugs are effective in the acute phase of the disease, although Bz shows a better safety and efficacy profile.[6] However, their efficacies are very low during the chronic phase.[7] Furthermore, these compounds have severe side effects, including anorexia, vomiting, peripheral polyneuropathy and allergic dermopathy.[8] The presence of nitro groups attached to the heterocyclic rings suggests that these drugs act on the parasite by nitro reduction, providing reduced intermediates that covalently modify biomolecules. However, their mode of action is currently under discussion.[9] Their high toxicity in humans is probably the result of oxidative or reductive tissue damage and is inextricably linked to their antiparasitic activity.[5] Recently, it has been proposed that the toxicity of these drugs could be linked to their microsomal nitroreduction to reactive metabolites inside the liver.[10] Therefore, existing drug treatments for CD are far from satisfactory and the development of a vaccine is a goal yet to be achieved. The discovery of low-cost new drugs circumventing the drawbacks of conventional drugs seems to be an urgent necessity.[4]

Research into antichagasic agents is mainly focused on biochemical metabolic key pathways or crucial parasite-specific enzymes. Sterol metabolism, kinetoplast DNA linked-sites, trypanothione reductase, cysteine proteinase,

hypoxanthineguanine phospho-ribosyltransferase, dihydrofolate reductase, and glyceraldehyde 3-phosphate dehydrogenase have fed the main lines of investigation during last years.[11]

Among the trypanosomatid-specific enzymes, we have focused our attention on iron superoxide dismutase (Fe-SOD). This enzyme, not found in mammals which have only manganese and copper/zinc superoxide dismutases (Mn and Cu/Zn-SOD), plays an essential role in the defence of the parasite against oxidation generated by the host immune system.[12] Indeed, it has been shown that parasitic protozoan survival is closely related to the ability of Fe-SOD to evade toxic free radical damage originated by their hosts.[13] Because of the predominant role of the prostetic groups, interaction with Fe-SOD active sites could be an efficient way of deactivating the antioxidant effect of the enzyme.

Regarding this point, in the last few years, our research group has designed a new family of polyamine compounds consisting of a macrocyclic pyridinophane core substituted with side chains containing additional donor atoms (Figure 1).[14] These macrocycles are termed *scorpiand ligands* since the side chain can fold towards the macrocyclic core following the binding of target guest species such as protons, anions or metal ions.[14,15]

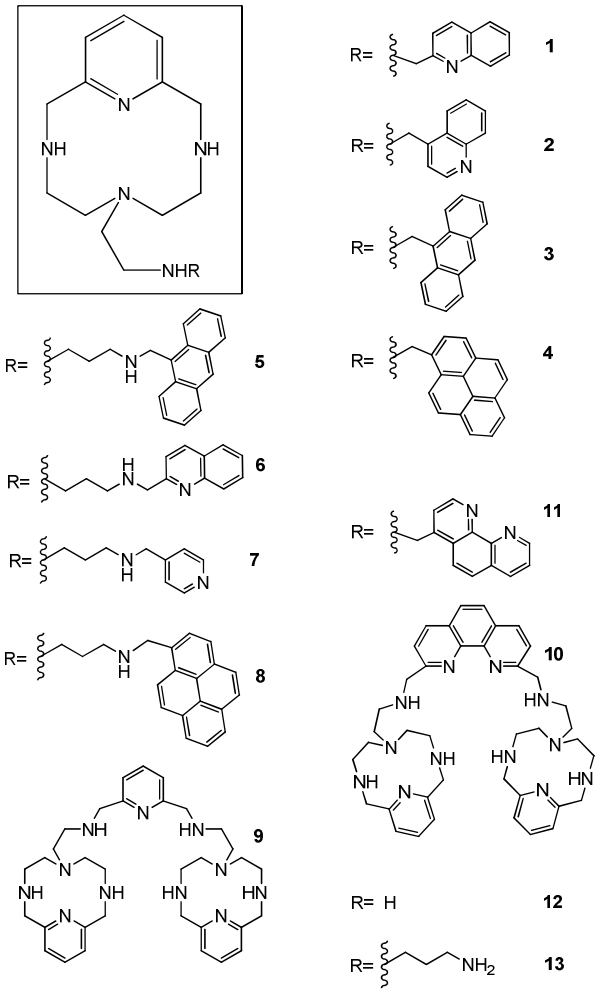

Figure 1. Chemical formula of aza-scorpiand derivatives. The common core for compounds 1-8 is depicted in the square.

Recently, we have studied the *in vitro* action of several of these compounds against *Trypanosoma cruzi* and two species of *Leishmania* (*L. infantum* and *L. braziliensis*). The results showed that the synthetic aza-scorpiand-like macrocyclic derivatives are potentially promising agents for the treatment of trypanosomatid infections.[16] In the present work, we tested the *in vitro* antiparasitic activity of 11 new polyaminic compounds and their toxicity against Vero cells. We compared the new compounds with Bz as a reference drug. Then, we chose the compounds with the best selectivity indices for the *in vivo* assay of the trypanocidal activity tests in the acute and chronic phases using female BALB/c mice as an animal model. The effect of the compounds on the ultrastructure of *T. cruzi* was also studied by transmission electronic microscopy (TEM) experiments to confirm the type of damage caused to the parasite. ^{1}H-NMR analysis of the nature and percentage of excreted metabolites was performed to obtain information about the inhibitory effect of our compounds on the glycolytic pathway since this represents the prime energy source of the parasite. Moreover, in order to check for metabolic disturbances or abnormalities associated with treatment, representative biochemical parameters were measured for all groups of mice.

Previously, we have demonstrated that these derivatives are good inhibitors of Fe-SOD, not only in *T.* cruzi,[16b] but also in *Leishmania spp*.[16a] An evaluation of their effectiveness as putative inhibitors of Fe-SOD in relation to human CuZn-SOD and also of trypanothione reductase is presented. Finally, an exhaustive molecular dynamic study was carried out to envisage the way in which these drugs approach and inhibit the active centre of Fe-SOD.

Results and discussion

Chemistry.

Synthesis of the compounds. The synthesis of **1**, **2**, **3**, **4**, and **11** was accomplished as described previously [14,17] following a modification of the Richman-Atkins procedure.[18] First, pertosylated polyamine tris(2-aminoethyl)amine (tren) was reacted with 2,6-bis(bromomethyl)pyridine in a 1:1 molar ratio using K_2CO_3 as the base in refluxing CH_3CN; this led to tosylated compound **12**. Detosylation was carried out with HBr/HAc/PhOH, obtaining **12** as a hydrobromide salt. Compounds **1**, **2**, **3**, **4** and **11** were obtained by reacting **12**, in its free amine form, with the corresponding carboxaldehydes (Scheme 1) in dry ethanol followed by *in situ* reaction with sodium borohydride. The compounds were finally precipitated as hydrochloride salts.

Compound **13** was obtained by the reaction of pertosylated polyamine **12** with N-(3-bromopropyl)phthalimide in a 1:1 molar ratio using K_2CO_3 as the base in refluxing CH_3CN. Deprotection and detosylation were carried out with hydrazine monohydrate and HBr/HAc/PhOH, respectively, obtaining **13** as a tetrahydrobromide salt.[17a] Compounds **5**, **6**, **7** and **8** were obtained by reacting **13**, in its free amine form, with the corresponding carboxaldehydes (Scheme 1) in dry ethanol followed by in situ reaction with sodium borohydride. The compounds were finally precipitated as the hydrochloride salts.[17a,19]

The synthesis of **9** and **10** was carried out by reacting two moles of **12** with one mole of pyridine-2,6-dicarboxaldehyde or 1,10-phenanthroline-2,9-dicarboxaldehyde, respectively, in dry ethanol, followed by *in situ* reduction with sodium borohydride. The compounds were finally precipitated as their hydrochloride salts.[17b]

Journal Name

RSCPublishing

ARTICLE

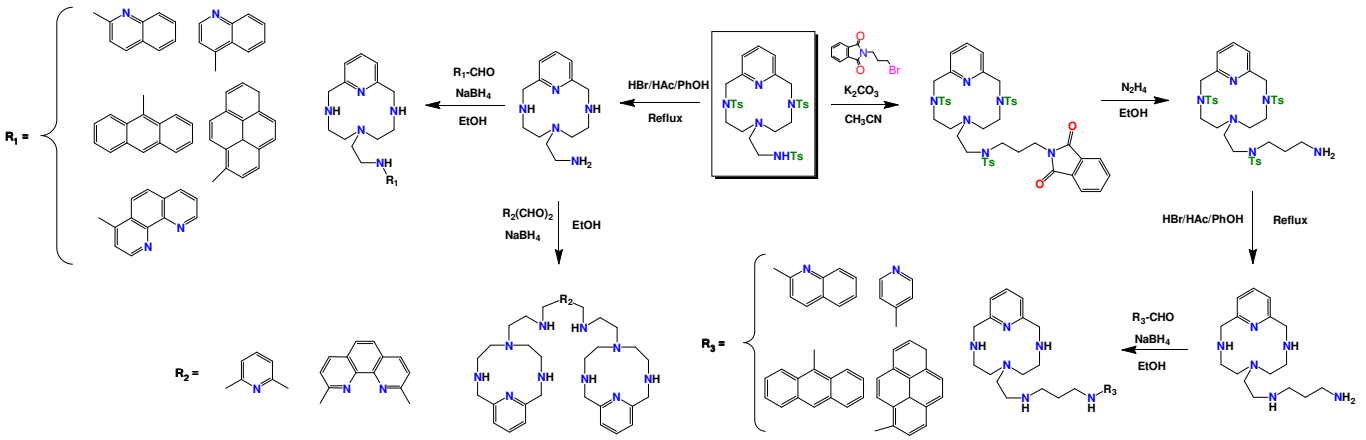

Scheme 1. Synthetic route for the preparation of compounds **1**-**13**.

Degree of protonation of the compounds. An important parameter that must be taken into account when dealing with polyamines is their acid-base behaviour. The protonation state of the amine groups in the macrocycle affects their interaction with other substrates since it defines their donor capabilities and their behaviour as hydrogen bond donors or acceptors. Table S1 presents the protonation constants determined by potentiometric titrations using 0.15 M NaCl as ionic strength. As can be seen in the Table, the number of protonated species corresponds with the number of secondary or primary amino groups present either in the macrocyclic core or in the arms. Protonation of the tertiary amines or pyridine groups was not observed, at least in the 2.0-11.0 pH range of the potentiometric titrations. Only in the case of the two macrocycles containing a phenanthroline unit and of the macrocycle with a 4-pyridine unit in their arms (**10**, **11** and **7**, respectively) was a further protonation step inferred.

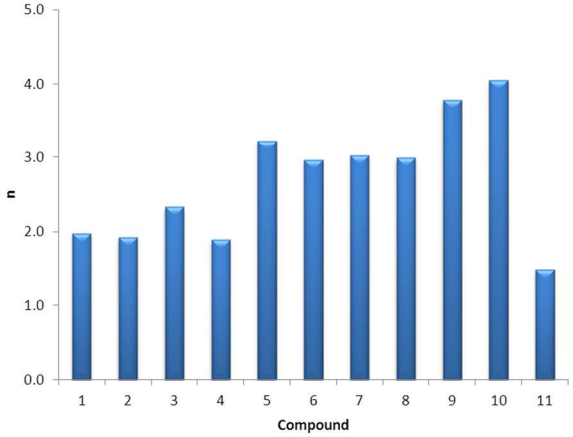

Figure 2. Protonation degree of the different compounds at pH 7.4.

An interesting point for this discussion and for the posterior molecular dynamics study is to know the protonation degree of the compounds at pH 7.4. Such data are plotted in Figure 2; it can be seen that while all the simple non-enlarged aza-scorpiands **1**-**4** and **11** had protonation degrees of ca. 2, the enlarged scorpiand molecules **5**-**9** reached a protonation degree of 3. Tritopic macrocycles **9** and **10** were the most charged compounds, reaching a protonation degree of almost 4 at this pH. Previous NMR studies have shown that first two protons bind preferentially to the amino groups of the macrocyclic core of **1**-**4** and **11**.[17b] The first three protons binding to **5**-**9** involve, apart from the two secondary amino groups of the core, one of the amine groups of the lateral chain.[14]

Interaction with iron. Since one of the potential targets of the studied compounds was the Fe-SOD of the parasites, it seemed interesting to evaluate the affinity of these chelating ligands for iron either in its II or III oxidation state. In Table S2, we present estimates of the binding constants for **1**, **2** and **7** as representatives of this series. As can be seen, all three compounds form stable complexes with either Fe(II) or Fe(III); the stability of the latter ones was remarkable and comparable to that found for the Cu^{2+} complexes previously described by some of us.[14,17,19] However, the stability of the Fe(III) complexes was not high enough to avoid the formation of hydroxo species and of Fe(III) hydroxide at basic pH values. On the other hand, Fe(III) systems might have been affected by side oxidation of amine groups to imines and, therefore, the stability constants are presented as tentative values. Anyway, in view of the distribution diagrams collected in Figure 3 and S1, it is clear that if the ligands approach the active site of Fe-SOD quite closely, some competition might be established with the primary ligands of the active centre for the capture of the metal ions.

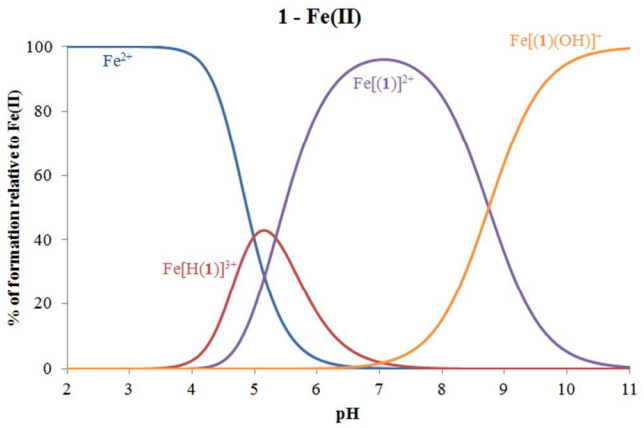

Figure 3. Distribution diagrams of the Fe(II)-**1** systems.

Biological Activity

In vitro trypanocidal evaluation. The *in vitro* activity of compounds **1–11** was evaluated against extracellular (epimastigote and trypomastigote) and intracellular (amastigote) forms of *T. cruzi*, as described in the Experimental Section. More indicative data were found with the assays performed on the intracellular amastigote forms, since epimastigotes are not the fully developed parasitic forms in vertebrate hosts. Finally, the compounds were tested against blood trypomastigotes, since these parasitic forms, along with the amastigotes, are responsible for the chronic phase of CD.
The IC_{50} values obtained for the extracellular and intracellular forms are shown in the first three columns of Table 1, which includes the data obtained for the reference drug Bz. Toxicity values were calculated against mammalian Vero cells after 72 h of culture and the selectivity indices (SI, calculated as IC_{50} Vero cells toxicity/IC_{50} activity of extracellular or intracellular forms of the parasite) are shown in the last three columns of Table 1. The numbers in brackets show the SI of the compound relative to that of Bz. This value indicates the *in vitro* potential of the test compounds with respect to the reference drug.

All compounds showed activity against the three parasite stages, and some of them were more active than Bz. Regarding the cytotoxicity against Vero cells, the compounds were substantially less toxic than the reference drug (see the IC_{50} values in Table 1). Considering the more illustrative selectivity index, compounds **1**, **2, 7,** and **11** were of potential interest with SI values 25 to 77-fold higher than those of Bz (Table 1). The SI values of the other compounds were lower, indicating that they are less suitable. However, when we checked the Mn^{2+} complexes of compounds **1** to **7** and **11**, a lower effect was observed (see Electronic Supplementary Information Table S3). This can probably be attributed to the protective effect that the Mn^{2+} complexes of these ligands exert over free radicals generated in the oxidative metabolism.[20]

Significant differences were found, however, in the unspecific cytotoxicity against Vero cells and, of course, in the selectivity indices (SI) resulting from these data. Despite this, there was not a clear relationship between toxicity and structure, and the more toxic compounds appeared to be the double scorpiands (**9**, **10**) and the single scorpiands containing large aromatic pyrene units (**4**, **8**). Taking into account all the data included in Table 1, compounds **1, 2, 7** and **11** were the best compounds, with **SI** values exceeding by 50 times or more those of Bz, depending on the parasite stage. According to some authors, only compounds with SI values exceeding 50 times the SI value of Bz are good enough to be considered interesting as antiparasitic drugs.[21]

Before starting the *in vivo* analysis of compounds **1**, **2**, **7** and **11**, an infectivity assay was performed. In such an assay, which is an *in vitro* reproduction of the life cycle of the parasite (see Electronic Supplementary Information, Infectivity section and Figure S2), it can be observed that all four selected compounds decreased the infection rate, i.e. by 73, 68, 82 and 76%, respectively. In the same way, they decreased the number of amastigote forms per infected cell at rates higher than 50%; consequently, the release of trypomastigote forms into the media decreased to 60, 44, 80 and 69%.

In vivo activity of scorpiand-like azamacrocyclic derivatives. The promising results obtained for the *in vitro* tests prompted us to study the *in vivo* activity of compounds **1, 2, 7** and **11** in a murine model (BALB/c mice).

The effectiveness of drugs currently in use against Chagas disease varies widely between the acute and chronic phases. Therefore, we decided to evaluate our compounds in both phases. For acute phase experiments, we considered the first 40 days after infection, whereas the effect on the chronic phase was studied between days 40 and 120 after infection for those compounds with high efficiency during the acute phase.

Scheme S1 in the ESI file provides a picture of all the *in vivo* experiments performed. The intraperitoneal administration route was preferred to the intravenous procedure because intraperitoneal treatment substantially reduces animal mortality.[22]

Table 1. In vitro activity, toxicity and selectivity index found for the aza-scorpiand-like macrocyclic derivatives on the extracellular and intracellular forms of *T. cruzi*.

Compound	IC_{50} (μM)[a]			Toxicity IC_{50} Vero Cell (μM)	SI[b]		
	Epimastigote forms	Amastigote forms	Trypomastigote forms		Epimastigote forms	Amastigote forms	Trypomastigote forms
Bz	16.2±0.8	23.6±0.7	22.6±0.8	13.6± 0.9	0.8	0.6	0.6
1	3.3±0.5	6±1	5±2	187±14	57 (71)	31 (52)	37 (62)
2	4.2±0.7	3.2±0.5	5±1	146± 9	35 (44)	46 (77)	29 (48)
3	16±2	13±2	22±3	214±15	13 (16)	16 (27)	10 (17)
4	3.2±0.3	4.2 ±0.3	7.4±0.7	83± 5	26 (33)	20 (33)	11 (18)

5	18.0±0.5	14±1	33±2	131±13	7 (9)	9 (15)	4 (7)
6	16±1	8.4±0.7	27±2	88±6	6 (8)	10 (17)	3 (5)
7	3.3±0.2	2.8±0.5	6.5±0.4	98±7	30 (38)	35 (58)	15 (25)
8	29±2	25±3	19.4±0.8	84±10	3 (4)	3 (5)	4 (7)
9	4.8±0.5	5.1±0.4	9±1	76±5	16 (20)	15 (25)	8 (13)
10	4.1±0.6	3.6±0.1	9.2±0.8	94±6	23 (29)	26 (43)	10 (17)
11	7.9±0.6	5.2±0.3	12±1	202±11	26 (33)	39 (65)	17 (28)

The values are the average of three separate determinations. [a]**IC_{50}** = the concentration required to give 50% inhibition, calculated by linear regression analysis from the values at the concentrations employed (1, 10, 25, 50 and 100 µM). [b]Selectivity index =IC_{50} Vero cells/IC_{50} extracellular or intracellular form of the parasite. In brackets: number of times that compound exceeds the reference drug SI (for the extracellular and intracellular forms of *T. cruzi*)

In fact, none of the animals died in any of our experiments performed either with the control or with **1, 2, 7** and **11** at the concentrations used (5 mg/kg of body mass). Female mice were inoculated with trypomastigotes, as described in the experimental section. Treatment, via the intraperitoneal route (i. p.), with the compounds of interest began 5 days post-infection (pi) and was maintained for an additional 5 days. Another group of mice was treated in the same manner, but with only the vehicle (control). During the study of acute phase activity, the levels of parasitaemia were determined every 2 days. Figure 4 shows the number of trypomastigote forms found in the blood until day 40 pi. On the days of maximum parasitic burden (peak days, 16-22 days pi) all compounds greatly reduced the number of circulating parasites. Furthermore, this reduction lasted until day 40 and was more significant for the groups treated with the compounds under study than for those treated with Bz. The order of *in vivo* activity towards the trypomastigote forms in the acute phase was: **7** > **11** > **2** >> **1** > Bz.

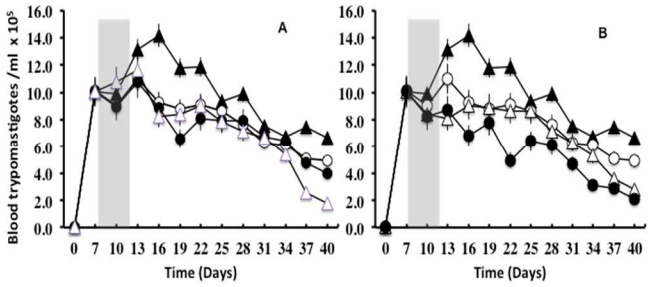

Figure 4 Parasitaemia in the murine model of acute Chagas disease (A and B): (-▲-) Control and dose receiving 5 mg/kg of body mass dose of: (-○-) Bz; in A: (-●-) compound **1**; (-Δ-) compound **2**; in B: (-●-) compound **7**; (-Δ-) compound **11**. All compounds were administered by the i.p. route. Grey shading represents the treatment period. Values are the means of six mice +/- standard deviation.

Compounds **1** and **2** showed moderate activity, since between 30 and 63% of the parasites survived the treatment (Figure 4A), while **7** and **11** displayed the highest activity during the acute phase (parasitaemia reduction greater than 80% by the end of the acute phase), as shown in Figure 4B. So, in view of these results, the group of mice treated with compounds **7** and **11** were kept until day 120 pi under the same conditions.

The experiment was accomplished by an immunosuppression test on the treated and control mice at day 120 pi (late chronic phase, in which there are no parasites remaining in the bloodstream). Figure 5A shows the reactivation of parasitaemia after immunosuppression. The control group recovered its initial parasitaemia almost entirely, thus giving a reactivation of 100%. In contrast, mice treated with **11** showed a parasitaemia load of 60% relative to their previous burden, while mice treated with **7** displayed an even lower reactivation of only 50%.

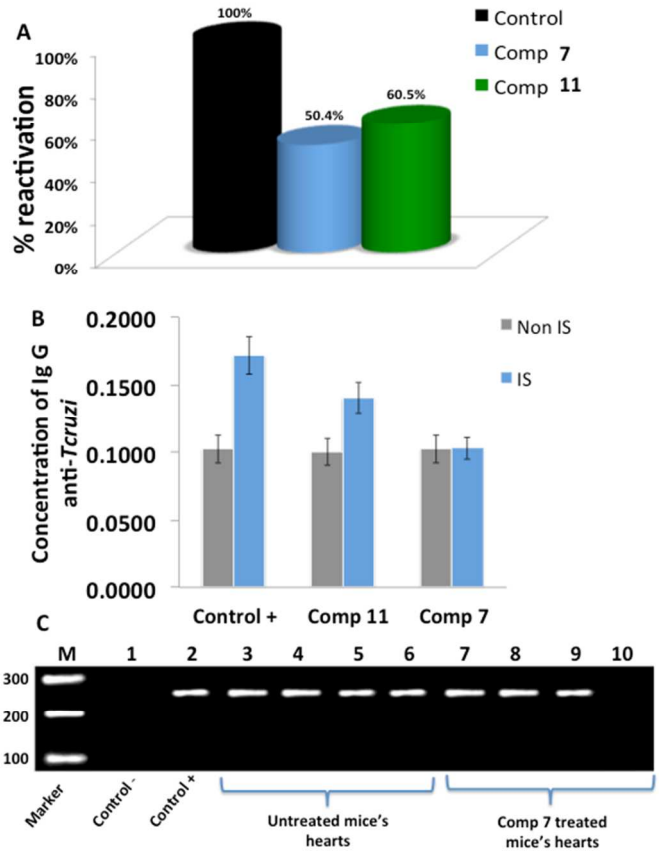

Figure 5 Immunosuppression experiment in the mouse model. (**A**) Reactivation of parasitaemia after immunosuppression. (**B**) Total IgG levels of anti-*T. cruzi*. Values are the means of three separate experiments and error bars represent the mean +/- standard deviation. (**C**) Polymerase chain reaction (PCR) analysis of heart tissue at the day 120 after infection. All mice from lane 3 to 10 were infected.

ELISA assays were used as an alternative method for verifying the effectiveness of these two compounds in the chronic phase after being challenged with an immunosuppression cycle. According to the literature, IgG titres in Balb/c become stable during the chronic phase of the disease;[23] this was confirmed in Figure 5B, which shows the anti-*T. cruzi* IgG levels. The IgG levels of the control group increased by about 40% due to the presence of parasites in the bloodstream after immunosuppression. However, the differences between immunosuppressed and non-immunosuppressed groups were smaller in the case of **11** and not significant for those treated with **7**. This means that the parasite-specific IgG level was not higher than the remaining amount of total unspecific level of IgG caused by the hypergammaglobulinaemia characteristic of infection with *Trypanosoma cruzi*.[23,24] Finally, Figure 5C shows the PCR

results after necropsy. The hearts were ground and underwent total DNA extraction and amplification of a fragment within the parasite SOD-gene. The hearts of control animals confirmed the presence of parasites, while the hearts of mice treated with **7** were relatively cleared from parasites (25% of the control value thus confirming the degree of curative effect of **7**.

We can conclude that the limited effectiveness of **7**, the best compound found in this study, was due to the low dosage used during the acute phase. Hence, we must take into consideration future experiments where we will increase the dosage and also modify the schedule of treatment for better exposure of the compound in the bloodstream. This increase in compound administration should not result in enhanced toxicity. Indeed, according to the data shown in Table S4, all the biochemical parameters tested regarding kidney, heart and liver profiles were maintained after compound administration; only the uric acid values showed an insignificant decrease of 10% (see the electronic supplementary information).

Molecular Mechanisms of Action

Metabolite excretion study. Since trypanosomatids are unable to completely degrade glucose to CO_2, they excrete a considerable portion of its hexose skeleton as partially oxidised fragments in the form of fermented metabolites, whose nature and percentage depend on the pathway used for glucose metabolism.[25] The catabolism products in *Trypanosoma cruzi* were acetate and succinate, with smaller percentages of L-alanine and D-lactate, in agreement with data in the literature.[26] The detection of large amounts of succinate as a major end product is a usual feature, because it relies on glycosomal redox balance, enabling re-oxidation of NADH produced in the glycolytic pathway. Succinic fermentation requires only half of the phosphoenolpyruvate (PEP) produced to maintain NAD+/NADH balance. The remaining pyruvate is converted inside the mitochondrion and the cytosol into acetate, D-lactate, L-alanine, or ethanol according to the degradation pathway followed by each species.[27]

To obtain some information about the effect of the tested compounds on parasite glucose metabolism, we registered the ^{1}H NMR spectra of *T. cruzi* epimastigote forms after treatment with **1, 2, 7** and **11**. The final excretion products were identified qualitatively and quantitatively (spectra not shown). The results were compared with those obtained from parasites maintained in a cell-free medium (control) for 96 hours. The characteristic presence of acetate, succinate, D-lactate and L-alanine was confirmed in the control experiments. As expected, succinate and acetate were the most abundant end products identified. However, after treatment of the parasites with the selected compounds, the excretion of catabolites was substantially altered at the dosages employed. Figure 6 shows the changes observed compared to the control. Remarkable differences in the catabolic pathway were observed, depending on the compound used, which seemed to be connected with the trypanocidal activity described above. The main features found were substantial decreases in succinate and lactate and, to a lesser extent, alanine. The most active compounds **7** and **11** decreased succinate, D-lactate and L-alanine by -28.4%, -39.7% and -22.1% and -28.4%, -27.0% and -23.7%, respectively.

All these data can be interpreted on the basis of a change in the succinate, D-lactate, L-alanine pathways occurring in the presence of the most active compounds **7** and **11**. It is well-known that D-lactate and L-alanine originate from the transformation of PEP in pyruvate in the presence of pyruvate kinase or pyruvate phosphate dikinase.[24a] Therefore, it seems possible that **7** and **11** interact with pyruvate kinase enzymes, thereby modifying the glucose metabolism of the parasite at the pyruvate stage. On the other hand, it is interesting to note that the decrease in succinate observed with **7** and **11** could also be related to dysfunction of the mitochondria, due to the redox stress produced by inhibition of the mitochondrion-resident Fe-SOD enzyme.[28] This should result in a decrease in pyruvate metabolism and a consequent decrease in succinate produced in mitochondria. All these data point out that the severe modifications generated in organelles like glycosomes or mitochondria by **7** and **11** is the ultimate reason for the alterations observed in the excretion products of *T. cruzi*.

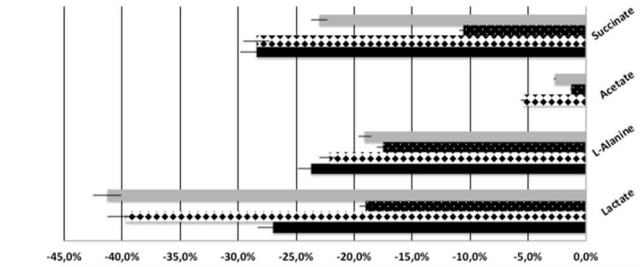

	Lactate	L-Alanine	Acetate	Succinate
Comp 1	-41,3%	-19,1%	-2,7%	-23,0%
Comp 2	-19,0%	-17,5%	-1,3%	-10,6%
Comp 7	-39,7%	-22,1%	-5,4%	-28,4%
Comp 11	-27,0%	-23,7%	0,0%	-28,4%

Figure 6. Variation percentages in the height of the peaks corresponding to metabolites excreted by *T. cruzi* epimastigotes in the presence of aza-scorpiand-like macrocycles derivatives at their IC_{25} compared to a control sample. Values are the means of three separate experiments and error bars represent the standard deviation.

Ultrastructural alterations. The trypanocidal activity shown by **1, 2, 7** and **11** should lead to relevant damage to parasite cells. Therefore, we performed a transmission electron microscopy (TEM) study on the epimastigote forms of *T. cruzi* treated with **1, 2, 7** and **11**. As expected, significant morphological alterations were observed when compared with untreated control cells (Figure 7). Without any doubt, the most effective compounds came out to be **7** and **11**, which caused considerable disturbances in many parasites. Compound **1** (Figure 7B) mainly caused disorganisation in the plasma membrane, enormous vacuoles inside, and mitochondria were found to swollen and expanded. The nuclei were also swollen and vacuolated, and in some parasites, the cytoplasm was full of reservosomes. More drastic effects were caused by **2**, as can be appreciated in Figure 7C, where some epimastigote forms were totally swollen with giant vacuoles which filled almost all the cytoplasm. Moreover, the mitochondria were disorganised and swollen, with small crystals and a less electron dense zone than usual that could be related to a loss of function. The parasites treated with compound **11** (Figure 7E) were totally disturbed, showing an empty cytoplasm, broken plasma membrane and some organelles were unrecognisable. Some similar alterations occurred when the epimastigote forms were treated with **7** (Figure 7D), where ribosomes were very few and the electron density was decreased in the nucleus. Mitochondria were swollen and microtubules were discontinuous along the cytoplasm.

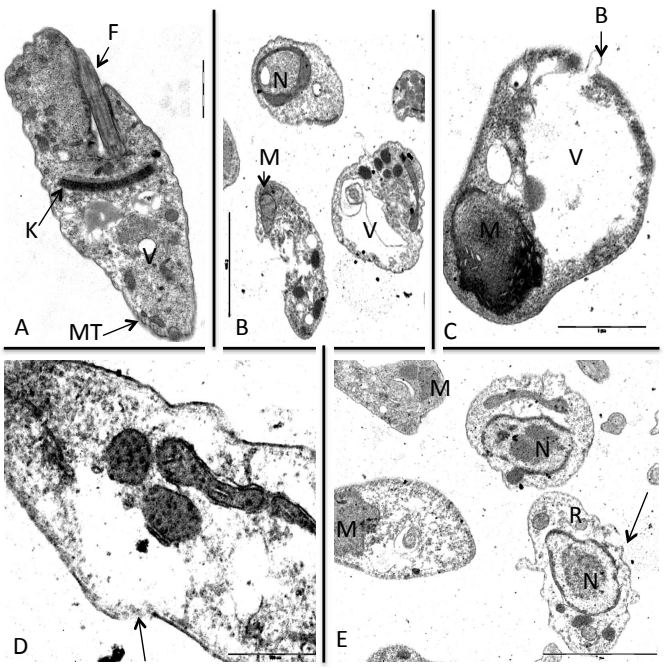

Figure 7. Ultrastructural alterations shown by TEM in epimastigotes of *T. cruzi* treated with aza-scorpiand-like macrocycles **1**, **2**, **7** and **11**. **A**, control parasite showing typical organelles such as nucleus (N), mitochondria (M), glycosomes (G), microtubules (MT), vacuoles (V), reservosomes (R), kinetoplast (K) and flagellum (F); **B**, treated with aza-scorpiand-like macrocycles **1**; **C**, treated with the compound **2**; **D**, treated with compound **7** and **E**, treated with compound **11,** at the IC_{25} concentration. Scale bar = 1µm.

Inhibitory effect on the T. cruzi Fe-SOD enzyme. These results prompted us to evaluate the inhibitory effect of **1**, **2**, **7** and **11** on Fe-SOD activity. The results are shown in Figure 8. Significant inhibitory values of Fe-SOD activity were found for the four compounds tested. Compounds **7** and **11** showed values close to 100% inhibition at 25-50 µM with IC_{50} values ranging from 4.2 to 6.6 µM. The design of an effective drug able to inhibit the parasite Fe-SOD without inhibiting human SOD is an interesting goal. Therefore, we also assayed the effect of these compounds on Cu/Zn-SOD from human erythrocytes. The results show that the inhibition percentages for human CuZn-SOD were lower than for Fe-SOD. The lead compounds **7** and **11** reached IC_{50} values of 98.0 and 55.8 µM for Cu-Zn-SOD, respectively.

It should be noted that, as mentioned above, these compounds not only showed greater alterations in glucose catabolism but they also led to greater levels of Fe-SOD inhibition. Since the Fe-SOD present in mitochondria is an essential part of the antioxidant protective response of the parasite, its inhibition would be related to a decrease in the rate of survival for the parasite. According to this fact, we hypothesise that compounds having a pyridine nitrogen on the side chain are able to get closer to the active centre of the enzyme, as is the case of compound **7**, so they might produce a greater inhibition. Modelling studies were carried out to obtain clues about this point.

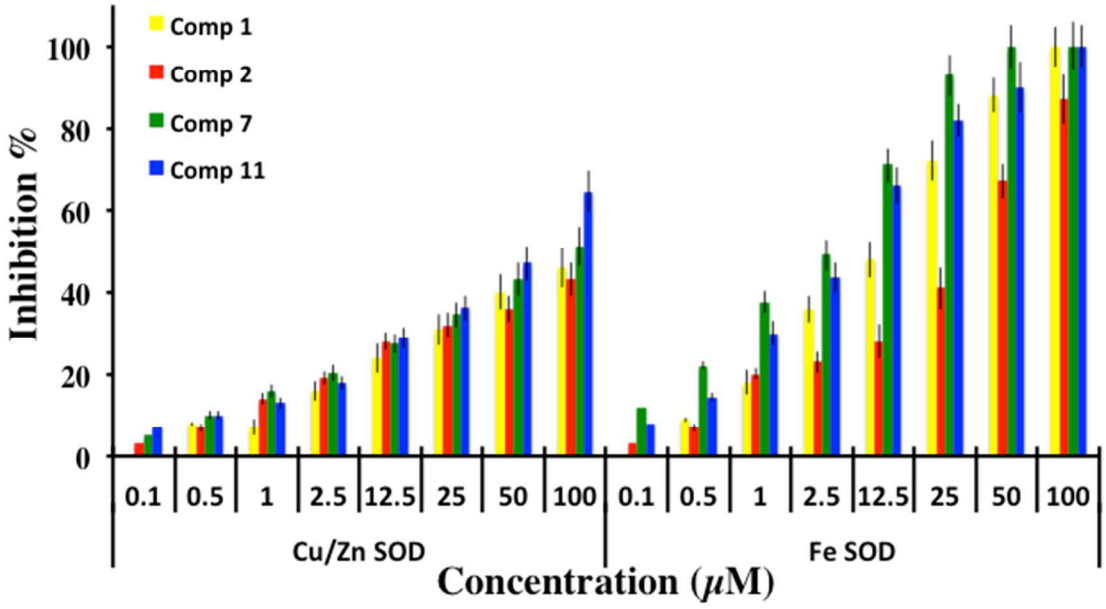

Figure 8. In vitro inhibition (%) of CuZn-SOD from human erythrocytes for compounds (activity 23.36/4.21 U/mg) and Fe-SOD from *T. cruzi* epimastigotes for compounds (activity 20.77/3.18 U/mg). x-axis represent the compound concentrations given for each enzyme. Enzyme concentration were kept constant in all assays. Differences between the activities of the control homogenate and those ones incubated with compounds were obtained according to the Newman-Keuls test. Values in the legend represent the IC_{50} = the concentration required to give 50% inhibition was calculated by linear regression analysis from the Kc values at the concentrations employed (0.1-100 mM).. IC_{50} values for Cu/Zn SOD = 123 µM; 172 µM; 98 µM and 56 µM, respectively for Comp 1, 2. 7, and 11. IC_{50} values for Fe SOD = 13 µM; 42 µM; 4 µM and 7 µM, respectively for Comp 1, 2. 7, and 11. Values are the average of three separate determinations and error bars represent the standard deviation

***Modelling studies*.** In order to learn about possible ways in which the compounds yielding the best trypanocidal activity inhibit the active centre of Fe-SOD, we carried out a molecular dynamics study in which the compounds were approached to Fe-SOD *T. cruzi* protein PDB_ID 2gpc. As commented with more detail in the experimental section, a distance restraint was applied between the heavy atoms of the active site residues and the heavy atoms of the compounds, using $\langle r^{-6} \rangle^{-1/6}$ average of all interaction distances to atoms of the groups. After the equilibration stage at 300 K, a total of 10 ns molecular dynamics was performed. Finally, the five minimum energy conformers were selected from the trajectory and minimised by removing all the restrains.

T. cruzi Fe-SOD is a dimeric protein with the polypeptidic chains constituted by seven helical regions and three anti-parallel β-strands.[29] The substrates approach the active site through a funnel in which H31 and Y35 serve as the gateway and restrict the access of small molecules towards the active site (Figure 9). The metal ion is coordinated in trigonal bipyramidal geometry to H27, H75, D160 and H164 and to a water molecule or a hydroxide anion. A hydrogen bond network involving the gateway residues Y35 and Q71 and the water molecule or hydroxide ion directly bound to the metal facilitate proton exchange between the active centre and the exterior of the protein.[30] Apart from this, residues E163 and Y167 extend towards the surface of the protein and help stabilise the dimer through hydrogen bonding with E163 and H31 of the other unit, respectively[30,31] (see Figure S3, electronic supplementary materials).

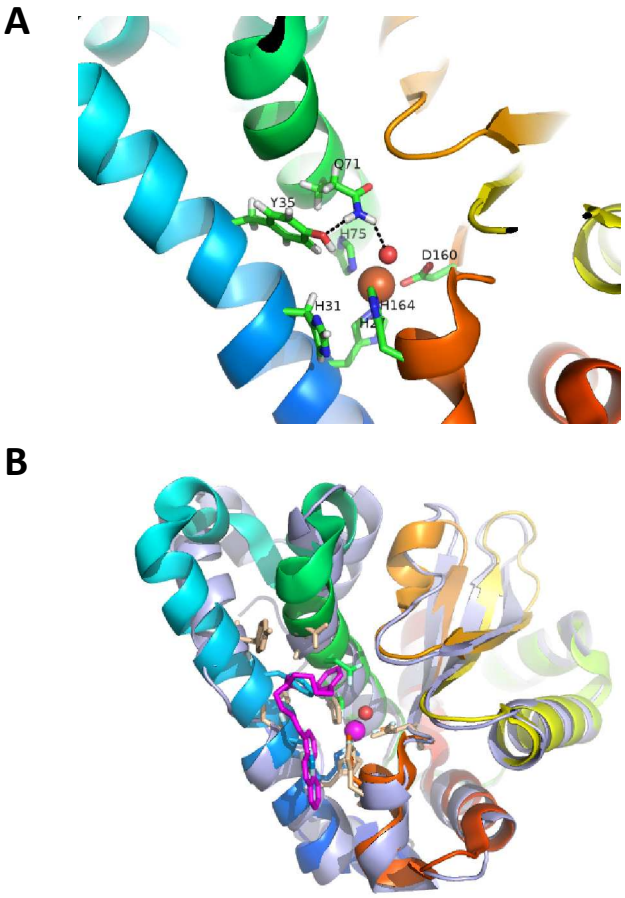

Figure 9. A) Representation of the active centre and residues forming the funnel gateway of Fe-SOD *Trypanosoma cruzi* protein PDB_ID 2gpc. Relevant hydrogen bond connections are presented as dotted lines. B) Cartoon representing the superimposition of the original 2gpc protein (rainbow colours) (only one chain) over the molecular dynamics minimum energy structure (pale blue) of the protein with compound **11** (magenta). Original residues have the corresponding rainbow colours while final dynamics residues are pale brown. Helices I are represented on the left.

The molecular dynamics studies with compounds **1**, **2**, **7** and **11** revealed profound changes in the active site environment. Although all the compounds examined displaced the gateway amino acids H31 and Y35, two different approaching orientations were identified. For **1**, **2** and **11**, the quinoline and phenanthroline subunits at the arm lie towards the exterior of the funnel while the macrocyclic core approaches the active centre, while for **7** the macrocycle is placed on the other way around, extending its lateral chain containing the 4-pyridine units towards the metal site and leaving the macrocyclic core oriented outwards. Although in none of these examples do the donor atoms of the inhibitors bind directly to the metal ion, they produce drastic changes in the hydrogen bond network around the active site at the time that they significantly alter helix 1 (see Figure 9B and Figure S4). Interestingly, the molecules approach the active site by taking advantage of a disrupted turn in the helix. The interaction of the compounds with the proteins pushes back the upper part of helix 1. As expected, all the compounds remove the hydrogen bond network formed by Y35 and Q71 and are involved in hydrogen bonding either with them or/and with H31. For instance, while **1** forms hydrogen bonds with Y35 and Q71, **11** establishes hydrogen bonds with H31 and Q71 (Figure S4).

In its turn, **2** makes hydrogen bonds with Q71 and also with H164, which forms part of the first coordination sphere of the metal ion lying the 4-quinoline unit parallel to the shifted Y35 of the gateway. Finally, in the case **7**, hydrogen bonds between the inhibitor and Y35 and H31 are observed while Q72 does not participate in the hydrogen bonding network. Additionally, **7** hydrogen also bonds to a leucine residue (L26). One surprising and very interesting result regards the way in which these molecules fit and close the funnel of the enzyme. As seen in the surface map of Figure 10, **11** (phenanthroline) completely occludes the funnel, preventing any other molecule from approaching the active site. The same event, although not to such a large extent, occurs for the other compounds (see Figure S5 in the ESI).

Trypanothione reductase (TR) inhibition assay. The best compounds were selected to evaluate their effects on *T. cruzi* trypanothione reductase (TR). All four compounds proved to be inhibitors of TR (Figure 11). At fixed concentrations of 40 and 100 μM for both the inhibitor and the substrate trypanothione disulphide (TS_2), the degree of inhibition varied between 14 and 89%. The most active *in vivo* trypanocidal compound **7** had the lowest inhibitory activity (lower than 50%), which renders TR unlikely as a potential target. The other three compounds **1**, **2** and **11** caused 74 to 89% inhibition when 100 μM of the compound and 40 μM of TS_2 were applied, indicating that they are inhibitors of the enzyme. Notably, no significant difference (around 10%) in the degree of inhibition at the two TS_2 concentrations was observed. This strongly indicates that these compounds do not act as pure competitive inhibitors.

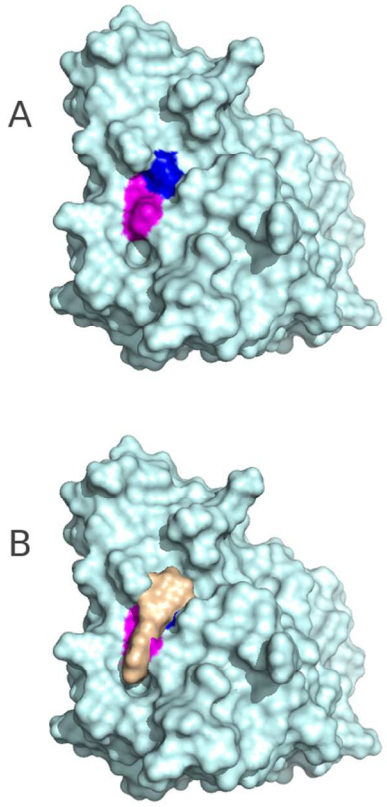

Figure 10. Solvent accessible surface of (A) original 2gpc protein and (B) 2gpc and minimised compound **11** (light brown) showing the occlusion of the funnel. H31 and Y35 are presented in magenta and blue, respectively.

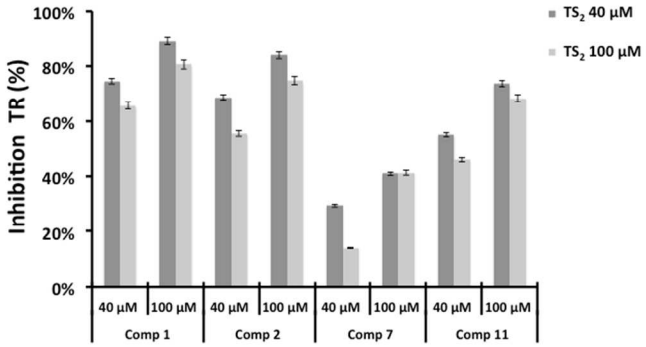

Figure 11. Inhibition of TcTR by compounds **1, 2, 7** and **11**. The activity was measured following the NADPH consumption at 340 nm as described in the Experimental Section. The control used to obtain 100% of activity was assayed without an inhibitor but rather the same amount of water used to dissolve the compounds. The values are average of two independent measurements Error bars show the standard deviation.

Trypanothione reductase kinetic study. To obtain insight into the molecular mode of action, the inhibitor constants and the type of inhibition were determined using Lineweaver–Burk plots, which revealed that all three compounds **1**, **2** and **11** behave as mixed type non-competitive inhibitors. Clearly, the lines cut in the double reciprocal plot above the x-axis.[32] In the case of **1**, Ki and Ki' values of 4 and 53 µM, respectively, were obtained. Compound **2** was slightly less efficient giving Ki and Ki' values of 8 and 114 µM. Finally, for **11**, the Ki and Ki' values were 16 µM and >200 µM (Figure 12). In any case, a higher affinity of the compound for the free enzyme compared to the enzyme-substrate complex was observed, as can be inferred from the calculated Ki < Ki' values.

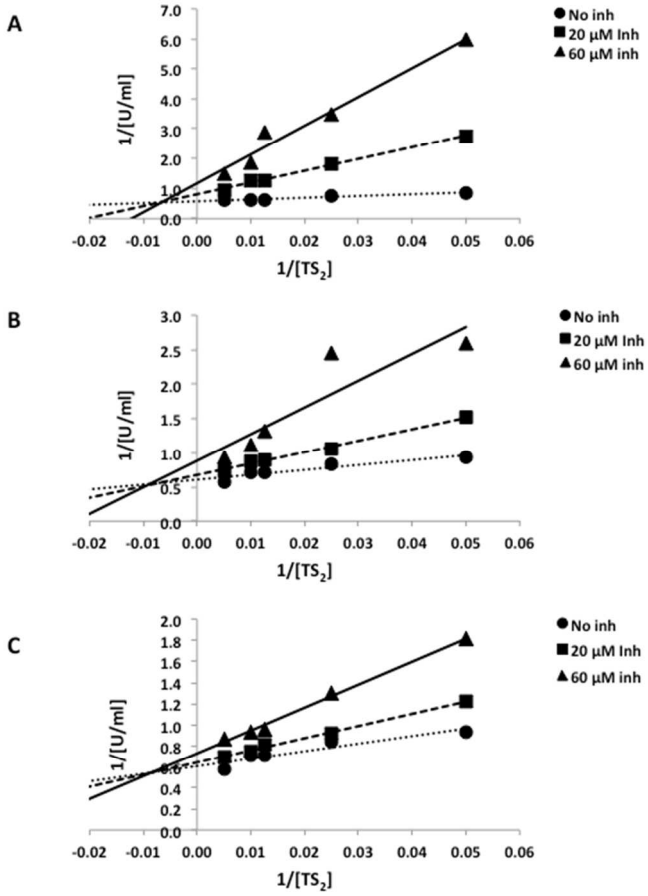

Figure 12. Lineweaver–Burk plots for the inhibition of TcTR by compound **1**(A), **2**(B), and **11** (C). The assays contained 100 µM NADPH and none, 20 µM, and 60 µM fixed concentrations of the inhibitor The TS_2 concentration was varied between 20, 40, 80, 100 and 200 µM.

In silico pharmacokinetic evaluation. Compounds **1**, **2**, **7** and **11**, which showed the best trypanocidal activity, were also submitted to an *in silico* pharmacokinetic properties evaluation. To evaluate the absorption rate, necessary for oral administration, we analysed the number of free rotatable bonds (n-ROTB) and Lipinski's "rule of five" for the lead compounds. Lipinski's descriptors evaluate the molecular properties for drug pharmacokinetics in the human body, especially for oral absorption. The rule states that the most "druglike" molecules present clogP ≤ 5, molecular weight ≤ 500, number of hydrogen bond acceptors (HBA) ≤ 10, and hydrogen bond donors (HBD) ≤ 5.[33] Lipinski's molecular descriptors and the predicted data of some ADMET properties of **1**, **2** (which share the same predicted values), **7** and **11** are summarised in Table 2. The predominant species at pH 7.4 (H_2L^{2+}, for **1**, **2** and **11** and H_3L^{3+} for **7**) was chosen for the evaluation. **1**, **2**, **7** and **11** showed acceptable n-ROTB values (≤10) and fulfilled Lipinski's rule of five. In addition, ADMET (absorption, distribution, metabolism, excretion and toxicity) properties were calculated using admetSAR (http://www.admetexp.org/),

a freely accessible web-based application.[34] The predicted data for BBB (blood–brain barrier) penetration and HIA (human intestinal absorption) were positive for all the tested compounds. Caco-2 cell permeability was negative in all cases, but with a moderate probability value. In the case of metabolism, various cytochromes P450 (CYP) were evaluated, showing similar patterns for all the compounds. In terms of toxicity, it was found that none of the compounds showed mutagenic toxicity with respect to the AMES test or carcinogenic effects.

Conclusions

The trypanocidal properties of a family of simple and double aza-scorpiand compounds, some of them newly synthesised, were examined both *in vivo* and *in vitro*. The experiments allowed us to select compounds displaying improved efficiency and lower toxicity than the reference drug. Parallel studies were carried out to establish the mechanism of action. Following this series of experiments, four compounds were selected as potential candidates to enter into clinical trials. Compounds **7** and **11** selectively inhibit the Fe-SOD enzyme of the parasites. Molecular dynamics studies indicated that these compounds block the access of substrates to the active site while they break the hydrogen bond pattern around the active site. Moreover, compound **7** showed an *in vivo* cure rate of 25% at a safe standard dosage of 5 mg/kg body mass. As shown by the NMR data, another mechanism of action of this series of compounds may be related to energetic mechanisms. On the other hand, **1** and **2** behaved as very effective trypanothione reductase (TR) inhibitors. The damage to the defence system of parasites produced by these compounds was reflected in the TEM ultrastructural analysis by high vacuolisation. Moreover, the compounds of choice displayed low *in vivo* toxicity, as reflected by the fulfilment of the ADMET rules. Finally, it deserves to be mentioned that, due to their different mechanisms of action, combined therapies should be further considered to obtain improved efficiency. A patent (P201330699) has already been filed for this family of compounds.

Table 2. Oral bioavailability, molecular properties and predicted ADMET properties of compounds **1**, **2, 7** and **11.**

	Compounds 1& 2		**Compound 7**		**Compound 11**	
	Result	Prob. (%)	Result	Prob. (%)	Result	Prob. (%)
Lipinski Molecular Descriptors						
HBA (≤10)	4		4		5	
HBD (≤5)	3		4		3	
clogP (≤5)	2.62		1.52		2.64	
MW (≤500)	393.56		400.59		444.61	
n-ROTB (≤10)	5		9		5	
Absorption						
BBB	+	87.9	+	67.7	+	87.9
HIA	+	72.2	+	74.1	+	72.2
Caco-2	-	61.6	-	65.9	-	61.6
Metabolism						
CYP450 2C9 substrate	NS	90.2	NS	89.8	NS	90.2
CYP450 2D6 substrate	S	63.0	S	55.9	S	63.1
CYP450 3A4 substrate	NS	77.0	NS	73.5	NS	77.0
CYP450 1A2 inhibitor	NI	89.5	NI	91.8	NI	89.5
CYP450 2C9 inhibitor	NI	96.0	NI	95.4	NI	96.0
CYP450 2D6 inhibitor	NI	69.5	NI	51.0	NI	69.5
CYP450 2C19 inhibitor	NI	95.1	NI	96.7	NI	95.1
CYP450 3A4 inhibitor	NI	90.0	NI	93.7	NI	90.0
Toxicity						
AMES toxicity	-	68.6	-	66.4	-	68.6
Carcinogens	-	93.2	-	93.9	-	93.2

[a] n-ROTB, number of rotatable bonds; HBA, number of hydrogen bond acceptors; HBD, number of hydrogen bond donors; clogP, logarithm of compound partition coefficient between n-octanol and water; MW, molecular weight; BBB, blood-brain barrier; HIA, human intestinal absorption; S, substrate; NS, nonsubstrate; I, inhibitor; NI, noninhibitor.

Experimental

Chemistry

The ESI contains the synthetic procedure for compounds **2** and **4** prepared for the first time and the characterisation data (NMR, mass spectrometry and elemental microanalysis) of all the compounds. Details of the potentiometric titrations, calculation of acid-base and stability constants and molecular modelling studies are also included in the ESI.

Biological activity – *in vitro* assays

The parasites and mammalian cells used are described in the electronic supplementary information. The procedures to test the different compounds against all parasite forms and mammalian cells individually as well as the infectivity assay, which represents a reproduction of the life cycle *in vitro*, are also provided.

Biological activity – *in vivo* assays

Mouse infection and treatment. This experiment was performed using the rules and principles of the international guide for biomedical research in experimental animals and with the approval of the ethical committee of the University of Granada, Spain. Groups of six BALB/c albino female mice (6–8 weeks old, 25–30 g weight), maintained under a 12-h dark/light cycle (lights on at 07:30 h) at a temperature of 22 ± 3 °C and provided with water and standard chow *ad libitum*, were inoculated via the intraperitoneal route with 5 x 10^5 blood trypomastigotes of *T. cruzi* obtained from previously infected mice blood. The animals were divided as follows: **I**, positive control group (mice infected but not treated); **II**, study group (mice infected and treated with the compounds under study). The administration of the tested compounds began on the seventh day of infestation once the infection was confirmed, and doses of 25 mg/kg body weight per day were administered for 5 consecutive days (7–12 days post-infection) by the intraperitoneal route. Peripheral blood was obtained from the mandibular vein of each mouse (5 µL samples) and dissolved in 495 µL of a PBS solution at a dilution of 1:100. The circulating parasite numbers were quantified with a Neubauer chamber for counting blood cells. This counting was performed every 3 days for 40 days (acute phase). The number of bloodstream forms found was expressed as parasites/mL. From this point onwards, the disease was considered chronic. The assays that follow are detailed in the ESI, where cyclophosphamide-induced immunosuppression and the assessment of cure are included.

Toxicity tests by clinical chemistry measurements. A fraction of the serum, obtained as shown above, was sent to the Biochemical Service at the University of Granada where a series of parameters was measured according to commercial kits acquired from Cromakit® using a BS-200 Chemistry Analyzer. Shenzhen mindray. Bio-medical electronics co., LTD. With the levels obtained for different populations of sera (n = 15, n = 6), we calculated the mean value and standard deviation. Finally, we also calculated confidence intervals for the mean normal populations based on a confidence level of 95% (100 × (1-α) = 100x (1-.05)%). The ranges obtained are shown in **Table S4**, which allows for the comparison and analysis of the sera studied in this work.

Studies on the mechanism of action:

Metabolite excretion study. Cultures of *T. cruzi* epimastigotes (initial concentration 5 × 10^5 cells/mL) received IC_{25} concentrations of the compounds under study (except for control cultures). After incubation for 96 h at 28°C, the cells were centrifuged at 400 g for l0 min. The supernatants were collected to determine the excreted metabolites using ^{1}H NMR. Chemical shifts were expressed in parts per million (ppm, δ scale), using sodium 2,2-dimethyl-2-silapentane-5-sulphonate as the reference signal. The chemical displacements used to identify the respective metabolites were consistent with those described previously.[35]

Ultrastructural alterations. The epimastigotes of *T. cruzi* were cultured at a density of 5 × 10^5 cells/mL in corresponding medium containing the compounds tested at their IC_{25} concentrations. After 72 h, these cultures were centrifuged at 400 g for 10 min, and the pellets were washed with PBS and then mixed with 2% (v/v) paraformaldehyde/glutaraldehyde in 0.05 M cacodylate buffer (pH 7.4) for 4 h at 4ºC. Following this, the pellets were prepared for transmission electron microscopy (TEM) study using a previously described technique.[36]

Superoxide dismutase (SOD) inhibition studies. The protocol to obtain the enzyme from the culture and the experimental measure of the inhibition assays are described in the ESI.

Trypanothione reductase (TR) inhibition studies. Recombinant trypanothione reductase from *Trypanosoma cruzi* (TcTR) was prepared following a published procedure.[37] TS_2 was generated enzymatically as described previously.[38] TR activity was measured in a total volume of 1 mL of 40 mM HEPES, 1 mM EDTA, pH 7.5, in the presence of 100 µM NADPH and varying concentrations of TS_2 (20, 40, 80, 100 and 200 µM) and/or inhibitor (0, 28 and 100 µM). The absorption decrease due to NADPH oxidation was followed at 340 nm and 25°C. Stock solutions of the inhibitors were prepared in water according to their solubility.

The K_i and K_i' -values were determined using the following equations:[32]

$$K_i = \frac{[I]}{\frac{K_{m(obs)}\left(1+\frac{[I]}{K_i'}\right)}{K_m} - 1}$$

$$K_i' = \frac{[I]}{\frac{V_{max}}{V_{max(obs)}} - 1}$$

The ability of the compounds to induce the oxidase activity of TR was measured in the presence of 100 µM NADPH, with 40 and 100 µM of the compound in a total volume of 1 mL and about 2 U/ml of TR. Under these conditions, spontaneous NADPH oxidation results in a minimal absorption decrease. This activity was not accelerated in the presence of the compounds, ruling out that they act as subversive substrates (data not shown).

Acknowledgements

Financial support for this study was received from the Spanish Ministry of Economy and Competitiveness (MINECO), CONSOLIDER-INGENIO 2010 CSD2010-00065 and Generalitat Valenciana PROMETEO 2011/008. F.O. is grateful for an FPU Grant from the Ministry of Education of Spain and he also thanks Natalie Dirdjaja and Dr Alejandro Leroux, Heidelberg, for their support with the kinetic analysis of TR.

Notes and references

[a] Departamento de Parasitología, Instituto de Investigación Biosanitaria ibs. Granada. Universidad de Granada, Granada, Spain. e-mail: msanchem@ugr.es
[b] Instituto de Ciencia Molecular, Departamento de Química Inorgánica, Universidad de Valencia, E-46980 Paterna (Valencia), Spain. e-mail: enrique.garcia-es@uv.es
[c] Departamento de Química Orgánica, Universidad de Valencia, E-46100 Burjassot (Valencia), Spain.
[d] Departamento de Química Física, Universidad de Valencia, E-46100 Burjassot (Valencia), Spain.
[e] Biochemie-Zentrum der Universität Heidelberg, Im Neuenheimer Feld 328, 69120 Heidelberg, Germany.
[†]Electronic Supplementary Information (ESI) available: [details of any supplementary information available should be included here]. See DOI: 10.1039/b000000x/
[‡]These authors have contributed equally to the work

1. P. J. Hotez, D. H. Molyneuz, A. Fenwick, J. Kumaresan, S. E. Sachs, J. D. Sachs, L. Savioli, *N. Engl. J. Med*. 2007, **357**, 1018–1027.
2. WHO, Global Report for Research on Infectious Diseases of Poverty, 2013, ISBN: 9789241564489.
3. WHO, Chagas disease (American trypanosomiasis), Fact sheet N°340, update March 2013**.**
4. A. M. Strosberg, K. Barrio, V. H. Stinger, J. Tashker, J. C. Wilbur, L. Wilson, K. Woo, *Institute for One World Health (IOWH)*: San Francisco, CA, 2007; 1–110.
5. J. A. Urbina, *Curr. Pharm. Designe.* 2002, **8**, 287-295.
6. R. Viotti, C. Vigliano, B. Lococo, M. G. Alvarez, M. Petti, G. Bertocchi, A. Armenti, *Expert. Rev. Anti-Infe.* 2009, **7**, 157-163.
7. C. J. Schofield, J. Jannin, R. Salvatella, *Trends. Parasitol.* 2006, **22**, 583-588.
8. (a) M. J. Pinazo, L. Guerrero, E. Posada, E. Rodríguez, D. Soy, J. Gascon, *Antimicrob. Agents. Chemother.* 2013, **57**, 390-395. (b) S. Cencig, N. Coltel, C. Truyens, Y. Carlier, *Int. J. Antimicrob. Agents*. 2012, **40**, 527-532.
9. (a) J. D. Maya, D. K. Cassels, P. Iturriaga-Vasquez, J. Ferreira, M. Faúndez, N. Galanti, A. Ferreira, A. Morello, *Comp. Biochem. Phys. A.* 2007, **146**, 601-620. (b) S. R. Wilkinson, C. Bot, J. M. Kelly, B. S. Hall, *Curr. Top. Med. Chem.* 2011, **11**, 2072-2084.
10. M. D. Mecca, L. Bartel, J. Castro, *Hum. Exp. Toxicol*. 2013, **32**, 1305-1310.
11. M. N. Soeiro, S. L. de Castro, *Expert. Opin. Ther. Targets* 2009, **13** (1), 105–121.
12. (a) L. Piacenza, F. Irigoín, M. N. Alvarez, G. Peluffo, M. C. Taylor, J. M. Kelly, S. R. Wilkinson, R. Radi, *Biochem. J.* 2007, **403** (2), 323-334. (b) I. A. Abreu, D. E. Cabelli, *Biochim. Biophys. Acta* 2010, **1804**, 263-274. (c) A. F. Miller, *Curr. Opin. Chem. Biol.* 2004, **8**, 162-168.
13. (a) R. K. Mehlotra, *Crit. Rev. Microbiol.* 1996, **22** (4), 295–314. (b) J. A. Atwood, D. B. Weatherly, T. A. Minning, B. Bundy, C. Cavola, F. R. Opperdoes, R. Orlando, R. L. Tarleton, *Science* 2005, **309**, 473–476. (c) M. A. Muñoz-Fernández, M. A. Fernández, M. Fresno, *Immunol. Lett.* 1992, **33**(1), 35-40. (d) V. M. Costa, K. C. Torres, R. Z. Mendonça, I. Gresser, K. J. Gollob, I. A. Abrahamsohn, *J. Immunol.* 2006, **177** (5), 3193-3200.
14. B. Verdejo, A. Ferrer, S. Blasco, C.E. Castillo, J. González, J. Latorre, M. A. Máñez, M. G. Basallote, C. Soriano, E. García-España, *Inorg. Chem.* 2007, **46**, 5707- 5719.
15. V. Amendola, L. Fabbrizzi, C. Mangano, P. Pallavicini, *Acc. Chem. Res.* 2001, **34**, 488-493.
16. (a) C. Marín, M.P. Clares, I. Ramírez-Macías, S. Blasco, F. Olmo, C. Soriano, B. Verdejo, M.J. Rosales, D. Gómez-Herrera, E. García-España, M. Sánchez- Moreno, *Eur. J. Med. Chem*. 2013, **62**, 466-477. (b) F. Olmo, C. Marín, M. P. Clares, S. Blasco, M. T. Albelda, C. Soriano, R. Gutiérrez-Sánchez, F. Arrebola-Vargas, E. García-España, M. Sánchez-Moreno, *Eur. J. Med. Chem.* 2013, **70**, 189-198.
17. (a) M. Inclán, M. T. Albelda, J. C. Frías, S. Blasco, B. Verdejo, C. Serena, C. Salat-Canela, M. L. Díaz, A. García-España, E. García-España, *J. Am. Chem. Soc.* 2012, **134**, 9644 – 9656. (b) J. González, J. M. Llinares, R. Belda, J. Pitarch, C. Soriano, R. Tejero, B. Verdejo, E. García-España, *Org. Biomol. Chem.* 2010, **8**(10), 2367 – 2376.
18. (a) J. E. Richman; T. J. Atkins, *J. Am. Chem. Soc.* 1974, **96**, 2268-2270. (b) J. E. Richman, T. J. Atkins, W. F. Oetle, *Organic Synthesis*, J. Wiley & Sons: New York, 1988, **6**, pp 652. (c) B. L. Shaw, *J. Am. Chem. Soc.* 1975, **97**, 3856-3857.
19. M. Inclán, M. T. Albelda, E. Carbonell, S. Blasco, A. Bauzá, A. Frontera, E. García-España, *Chem. Eur. J*. 2014, **20**, 1 – 13.
20. M. P. Clares, S. Blasco, M. Inclán, L. del Castillo Agudo, B. Verdejo, C. Soriano, A. Doménech, J. Latorre, E. García-España, *Chem. Commun.* 2011, **47**, 5988- 5990.
21. S. Nwaka, A. Hudson, *Nat. Rev. Drug Discov.* 2006, **5**, 941-955.
22. C. F. Da Silva, M. M. Batista, D. G. J. Batista, E. M. de Souza, P. B. da Silva, G. M. de Oliveira, A. S. Meuser, A. R. Shareef, D. W. Boykin, M. N. C. Soeiro, *Antimicrob. Agents Chemother.* 2008, **52**, 3307-3314.
23. A. el Bouhdidi, C. Truyens, M. T. Rivera, H. Bazin, Y. Carlier, *Parasite Immunol*. 1994; **16**(2): 69-76.
24. M. A. Bryan, S. E. Guyach, K. A. Norris, *PLoS Negl. Trop. Dis*. 2010; **4** (7), e733.
25. F. Bringaud, L. Riviere, V. Coustou, *Mol. Biochem. Parasit.* 2006, **149**, 1-9.
26. J. Turrens, *Parasitol. Today* 1999, **15**, 346-348.
27. P. A. M. Michels, F. Bringaud, M. Herman, V. Hannaert, *Biochim. Biophys. Acta* 2006, **1763**, 1463-1477.
28. I. G. Kirkinezos, C. T. Moraes, *Cell & Developmental Biology* 2001, **12**, 449-457.
29. J. F. R. Bachega, M. V. A. S. Navarro, L. Bleicher, R. K. Bortoleto-Bugs, D. Dive, P. Hoffmann, E. Viscogliosi, R. C. Garratt, *Proteins* 2009, **77**, 26-37.
30. T. Hunter, K. Ikebukuro, W. H. Bannister, J. V. Bannister, G. J. Hunter, *Biochemistry* 1997, **36**, 4925-4933.
31. M. M. Whittaker, J. W. Whittaker, *J. Biol. Chem.* **1998**, 273, 22188-22193.
32. M. Dixon, E. C. Webb, *Logman Scientific & Technical: Harlow*, Essex, England, 1986.
33. C.A. Lipinski, F. Lombardo, B. W. Dominy, P. J. Feeney, *Adv. Drug Deliv. Rev*. 2001, **46**, 3–26.
34. F. Cheng, W. Li, Y. Zhou, J. Shen, Z. Wu, G. Liu, P. W. Lee, Y. Tang, *J. Chem. Inf. Model*. 2012, **52**, 3099-3105.
35. C. Fernández-Becerra, M. Sánchez-Moreno, A. Osuna, F. R. Opperdoes, *J. Eukaryot. Microbiol.* 1997, **44**, 523- 529.
36. I. Ramírez-Macías, C. Marín, R. Chahboun, I. Messouri, F. Olmo, M. J. Rosales, R. Gutierrez-Sánchez, E. Alvarez-Manzaneda, M. Sánchez-Moreno, *Am. J. Trop. Med. Hyg.* 2012, **87**, 481-488.
37. Sullivan, F.X.; Walsh, C.T. Cloning, sequencing, overproduction and purification of trypanothione reductase from Trypanosoma cruzi. *Mol. Biochem. Parasitol.* **1991**, 44(1), 145-147.
38. Comini, M.A.; Dirdjaja, N.; Kaschel, M.; Krauth-Siegel, R.L. Preparative enzymatic synthesis of trypanothione and trypanothione analogues. *Int. J. Parasitol*. **2009**, 39, 1059–1062

